Reactive Scattering Damage to DNA Components by Hyperthermal Secondary Ions

Zongwu Deng, Ilko Bald,† Eugen Illenberger,† and Michael A. Huels*

Ion Reaction Laboratory, Department of Nuclear Medicine and Radiobiology, Faculty of Medicine and Health Sciences, University of Sherbrooke, Sherbrooke, Quebec, J1H 5N4, Canada

(Received 28 February 2006; published 23 June 2006)

We have observed reactive scattering damage to fundamental DNA building blocks by the type of hyperthermal secondary ions that are produced along heavy ion tracks in biological media. Reactions include carbon abstraction by N^+, and hydrogen abstraction by O^- and N^+, at collision energies down to 1 eV. Our results show that localized reactive scattering by hyperthermal secondary fragments can lead to important physicochemical damage to DNA in cells irradiated by heavy ions. This suggests a fundamentally different picture of nascent DNA damage induced by heavy ion tracks, compared to conventional (x or γ) radiation tracks.

DOI: 10.1103/PhysRevLett.96.243203 PACS numbers: 34.50.Dy, 82.30.Fi, 87.14.Gg

Hadron therapy (proton and ions) has achieved significant clinical success in treatment of many dedicated tumors [1], e.g., deep-seated brain and skull base tumors [2] and eye melanomas [3], which benefits from its unique dose distribution. Heavy particles deliver radiation doses up to an energy-dependent depth with a maximum dose density deposited at the ''Bragg peak'' shortly before the track end. This unique dose distribution results in higher survival probability of healthy tissue along the radiation track before the Bragg peak, and spares the healthy tissue beyond [4,5]. Current models of hadron therapy are based on the assumption that it causes DNA damage via similar pathways as conventional ionizing radiation, involving mainly *simple ionization*, *single bond cleavage, and slow radical attack*, but modulated by its different track structure and higher ionization density [6,7]. However, contemporary studies have revealed that (a) along the radiation track of a primary heavy particle (MeV range), significant amounts of energetic secondary fragments (e.g., C^{n+}, O^{n+}, N^{n+}, $n = 1$–3) with *hyperthermal energies up to several hundreds of electronvolts* can be produced [8,9], and (b) these secondary ions can cause substantial direct physical (e.g., kinetic) damage to DNA components by inducing molecular fragmentation [10] at collision energies as low as 10 eV (0.25 eV/amu). This suggests that the difference between sparsely ionizing radiation (electrons and photons) and densely ionizing heavy ion tracks reaches beyond track structure and density, and may also be linked to the different hyperthermal secondary particles created along the ion tracks.

Another important aspect of heavy particles is the space radiation risk that mission crews encounter. At low earth orbit crews are mainly exposed to high energy electrons (up to 6 MeV) and protons (up to 250 MeV) trapped by the geomagnetic field [11]. During missions at high orbit, or beyond the geomagnetic field's protection (e.g., the lunar and Mars mission programs of NASA) the radiation risk arises predominantly from high energy and high mass particles in the GeV/nucleon range [11]. Such high linear energy transfer (LET) space radiation is considered the most mutagenic, or lethal due to their penetrating character. Current state-of-the-art risk estimates for exposure to space radiation essentially rely on empirical weighting factors for different heavy particles, and extrapolation from high dose rate, low LET data (e.g., Japanese atomic bomb survivors; human exposure to x and γ rays). This leads to serious uncertainties of several 100% in estimating, for example, long term biological effects on astronauts [12]. A major reason for these uncertainties is the persistent lack of basic knowledge concerning proton or heavy ion damage to biological systems at a molecular level. Because low LET radiation effects have been extensively studied from the macroscopic down to the molecular level, risk estimates for high LET radiations can be improved by acquiring similarly detailed knowledge of high and low LET radiation effects, not merely at the microscopic (cellular) level [13,14], but also on the nanoscopic scale of DNA and its basic subunits.

Here we show that physicochemical collision reactions between hyperthermal secondary ion fragments, such as those created by primary heavy ion tracks, and DNA components lead to significant molecular damage at collision energies as low as 1 eV, via atom (e.g., C and H) abstraction from the DNA sugar backbone subunits. These secondary hyperthermal ions are able to severely damage DNA components not only via direct collisional effects, but also through complex reactive scattering pathways. This suggests that the difference between high and low LET radiation tracks lies not only in the higher ionization density of ion tracks, but is also attributable to (a) the different hyperthermal secondary particles created along ion tracks, their higher energies, different reactivities, and different distribution along the track, and (b) the different physicochemical mechanisms responsible for DNA damage, which reach beyond simple ionization and bond cleavage, or diffusion-limited radical attack.

The experiments were conducted in the Sherbrooke laboratory on an ultra-high-vacuum ion beam system [10], which delivers a well focused, mass- and energy-resolved, positive ion beam in the 1–100 eV energy range

into a reaction chamber for sample irradiation. The energy of the ions is held fixed in this energy range and the energy spread of the beams is measured to be ~1 eV full width at half maximum over the entire energy range. Beams of ~70 nA N^+ and N_2^+ and ~30 nA Ar^+ ions, focused at the target to a 2–4 mm spot, are used in the present experiments. In the reaction chamber a quadrupole mass spectrometer (QMS) is installed perpendicularly to the ion beam axis to monitor desorbing cation and anion products *during* primary ion impact. The QMS measures desorbed ions with *in vacuo* energies between 0 and 5 eV. Multilayer films of DNA and RNA components [nucleoside thymidine (dT), base thymine (T), and sugar molecules D-ribose (R) and 2-deoxy-D-ribose (dR)] are prepared by *in vacuo* evaporation onto an atomically clean polycrystalline Pt substrate. The Pt substrate is cleaned by flash-heating near 1000 °C prior to each film deposition, and its cleanliness is verified by 200 eV Ar^+ secondary-ion mass spectroscopy. All compounds have stated purities of 99.5%.

Previously it was shown that Ar^+ ions can induce molecular fragmentation of these DNA components via kinetic and potential scattering at collision energies down to about 10–15 eV [10]. This is also observed here during N^+ and N_2^+ ion irradiation with similar fragmentation patterns [15]. The fragments of thymidine originate from both thymine and the sugar moiety, including H^+, CH_3^+, H_3O^+, $C_2H_3^+$, $HNCH^+$, CHO^+, CH_3O^+, $C_3H_3^+$, $HNC_3H_4^+$, $[T\text{-}OCNH]^+$, $[T\text{-}O]^+$, $[T+H]^+$, H^-, O^-, OH^-, CN^-, and OCN^-, etc. However, the majority of these fragments originate from the sugar moiety.

More importantly, however, here at collision energies *well below* 10 eV, reactive scattering is also observed. Nitrogen ions efficiently abstract hydrogen and/or carbon atoms from these molecules to form NH^-, NH_2^-, and CN^- anions. Figure 1 shows segments of the anion mass spectra produced by 5 and 15 eV N^+, and 40 eV N_2^+ irradiation. The spectra were acquired from films of ~1 monolayer thymine or thymidine, and ~20 monolayer 2-deoxy-D-ribose. The 15 amu anion is unambiguously assigned to NH^-, while the 16 amu anion produced by N^+ ion irradiation below 25 eV is assigned to NH_2^-, because here molecular fragmentation yielding O^- occurs only above 25 eV (see below). Note that NH^- and NH_2^- are only observed during N^+ irradiation of sugars (R and dR) and thymidine, but not for thymine. The 16 and 17 amu anions produced by 40 eV N_2^+ irradiation are attributed to O^- and OH^- fragments since no NH^-, and thus likely no NH_2^-, is produced for N_2^+ irradiation in the investigated energy range of 1–100 eV. The 26 amu anion is observed in all cases and unambiguously assigned to CN^-, because no $C_2H_2^-$ anion is observed during Ar^+ ion irradiation of R and dR. The use of thicker 2-deoxy-D-ribose films guarantees that the source of carbon in the formation of CN^- is from adsorbed molecules.

Figure 2 shows the product yields of NH^- and CN^- as a function of incident N^+ and N_2^+ ion energy during irradiation of the above films, with thresholds of CN^- desorption down to 5 and 30 eV, respectively. NH^- desorption is observed at energies down to 1 eV, suggesting an exoergic reaction. CN^- desorption during N_2^+ ion irradiation appears at much higher energies near 30 eV than for N^+ irradiation. This higher energy is required to break the incident N_2^+ ion into two atomic nitrogen, which then abstract carbon atoms from adjacent molecules to form CN^-. Because the ionic reaction product must possess sufficient kinetic energy to overcome a charge induced polarization barrier of about 1–1.5 eV at the surface of the film [16], the reaction is likely to continue at energies somewhat *below* the measured CN^- desorption threshold, yielding however products with kinetic energies insufficient for desorption. This is supported by the observation of carbon abstraction from graphite by nearly 0 eV N^+ [17]. This reaction is driven by the formation of a strong C≡N triple bond (7.8 eV) [17].

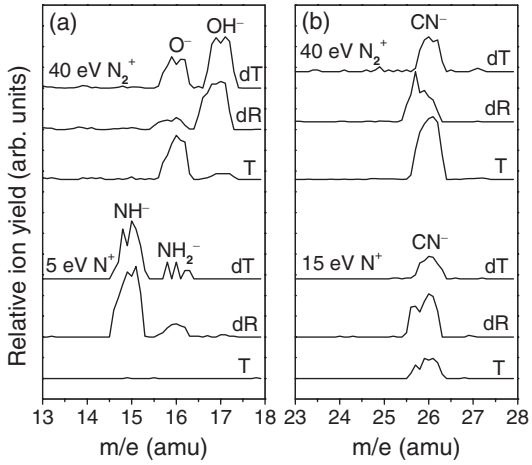

FIG. 1. Anion mass spectra showing the formation of (a) NH^-, NH_2^- and (b) CN^- during 5, 15 eV N^+ and 40 eV N_2^+ ion irradiation of T, dR, and dT films. The relative product yields have been vertically displaced for clarity. The result of R is similar to that of dR. CN^- desorption from ribose films (R and dR) is completely due to carbon abstraction, while its desorption from thymine and thymidine films above 25 eV also has contribution from molecular fragmentation (kinetic scattering).

Because the dissociation of N_2^+ gives rise to at least one neutral nitrogen atom, the absence of NH^- and NH_2^- during N_2^+ irradiation suggests that *neutral* nitrogen atoms are not the precursors of NH^- and NH_2^- formation, i.e., their formation during N^+ irradiation shows that it involves *ionic* nitrogen atoms. Furthermore, the appearance of NH^- and NH_2^- anions during N^+ irradiation of R, dR, and thymidine, and absence during irradiation of thymine (without hydroxyl group) suggest that they are a result of N^+ *ion* reactions with *hydroxyl* hydrogen in the molecules (However, here we cannot rule out that neutral nitrogen atom abstracts hydrogen to form neutral NH [18]). Thus, the absence of NH^- and NH_2^- anions during N_2^+ ion irradiation suggests that the collisional dissociation of N_2^+

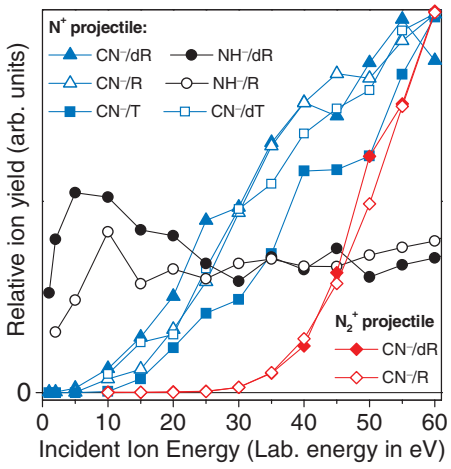

FIG. 2 (color). Desorption energy thresholds of NH^- and CN^- anions during N^+ and $N_2{}^+$ ion irradiation of dR , R, T, and dT films on Pt substrate. All CN^- ion yields are normalized in intensity at 60 eV, and the NH^- anion yields are normalized to ~ half of the CN^- maximum yield for ease of comparison.

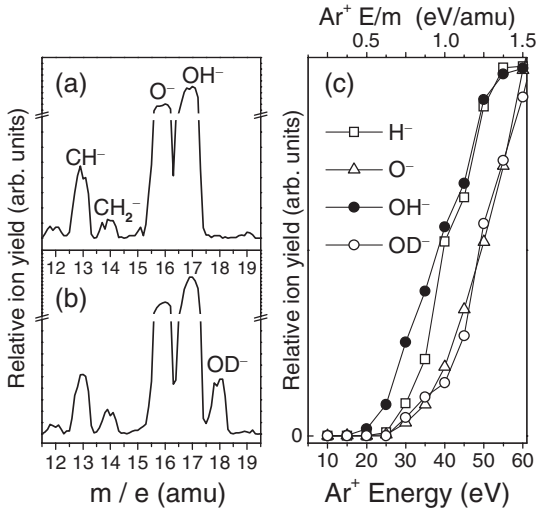

FIG. 3. Anion mass spectra obtained during 100 eV Ar^+ irradiation of (a) D-ribose and (b) 1D D-ribose showing the formation of OD^- anions. (c) Incident ion energy dependence of OH^-, H^-, O^- (from D-ribose), and OD^- (from 1D D-ribose) desorption during Ar^+ ion irradiation.

ions gives rise to two neutral nitrogen atoms [19]. Consequently, during $N_2{}^+$ ion irradiation the carbon abstraction reaction observed here likely involves *neutral* nitrogen atoms, i.e., this reaction can proceed with both ionic and neutral atomic nitrogen. In other words, *the charge state of atomic nitrogen is not critical in carbon abstraction*, unlike in hydrogen abstraction.

Hydrogen abstraction by secondary oxygen fragments is also observed here, as indicated by the formation of OD^- anions during ion irradiation of 1D D-ribose films (Cambridge Isotope Laboratories, 98% isotopic purity). Figure 3 shows desorption of OH^-, O^-, H^-, and OD^- anions during Ar^+ irradiation of (a) D-ribose and (b) 1D D-ribose films. Their dependence on incident Ar^+ ion energy is shown in Fig. 3(c). Ar^+ irradiation produces OH^- anions directly via breaking of carbon-hydroxyl bonds, which starts near 15 eV. With increase in incident ion energy, more violent collisions also lead to O-H bond cleavage to yield O^- or H^- anions at above 25 eV Ar^+ energies. The fact that OD^- ions appear at an energy higher than OH^-, but coincide with O^- formation suggests that it is not formed via carbon-hydroxyl bond breaking after inter- or intramolecular H-D exchange, but via D abstraction from C1 by either an oxygen atom or an O^- (not resolvable by present experiments). Similar reactions are also observed during (1) hyperthermal O^+ ion interaction with alkane films [20], and (2) low energy electron irradiation of films containing O_2 and tetrahydrofuran (THF), where dissociative electron attachment to O_2 molecules produces O and O^-; the latter abstracts H from THF to form OH^- [21]. This suggests that here *the charge state of* O *is not critical in the* H*-abstraction reaction*. Another observed secondary fragment reaction pathway is H_3O^+ formation [10,22].

The basic physical and physicochemical processes observed here suggests that the energetic secondary ions/neutrals produced along the track of a high energy heavy particle can cause substantial damage to cellular DNA in subsequent scattering events. As the present and previous experiments have shown [8–10,22], this will proceed via many different pathways (both physical and physicochemical), and can result in the complete destruction of DNA building blocks. The events are more violent and complex than in conventional radiation. While hydrogen abstraction is frequently observed during radiolysis of DNA in solution [23], carbon abstraction from DNA components by hyperthermal ions, *observed here for the first time*, can cause severe molecular damage to DNA components, e.g., destruction of the ring structures of base and sugar molecules. Particularly, when a nitrogen atom is knocked out from a DNA base by a primary ion *as either an ion or an atom*, it can efficiently abstract a carbon atom from an adjacent DNA subunit, as shown here. Specifically, abstraction of C3, C4, and C5 from the sugar moiety leads to, by definition, a single-strand break, and abstraction of C1 leads to a base loss. We also note that such *nonthermal* collision reactions occur at the picosecond stage following primary ion radiation, complete on time scales comparable to molecular vibrations, or collision times, viz. within 10^{-12}–10^{-14} s, and thus cannot be classified as ''ordinary'' chemical reactions due to their ballistic nature, unlike the later thermal diffusion-limited radiation chemical reactions [23].

Conventional low LET radiation induces damage mainly via simple ionization associated with the production of secondary electrons, radicals and ions [23,24]. Subsequent interaction of these secondary particles with the biomedium comprises the major biological damage [23–28]. Because the secondary radicals and ions have energies of typically well below 5 eV (at most 10–15 eV in cases of

core ionization), most of them can only travel within 1 nm from their formation site in a dense biological medium [24]; this is much below the minimum distance of ~2 nm required for the production of a second strand break on the opposite DNA strand, required for a double-strand break. Hence, in most cases, *mainly* single-strand breaks are generated by conventional low LET radiation.

The significantly more energetic secondary ions/neutrals produced along the tracks of heavy ions can scatter over distances of up to 5–10 nm, which allows them to reach the opposing phosphate-sugar backbone, but still remain within a distance of 10 base pairs from their formation site. As a consequence, complex and multiple molecular damage can be produced within a distance of several nm via subsequent collision events, so that biologically more lethal DNA damage such as double-/multiple-strand breaks and multiply damaged sites (damage clusters) can result, which are more difficult to repair than single-strand breaks [29]. Clustering of DNA damage can be further enhanced by the higher ionization density in the Bragg peak where the maximum energy density is deposited, and thus the majority of hyperthermal secondary particles are produced.

While the underlying mechanisms of heavy ion radiation damage to a biomedium appear more complex and varied than those induced by conventional low LET radiation, the resulting damage is likely to depend not only on the physical structure (ionization density), but also on the *chemical structure* of the heavy ion track: high energy heavy ion interactions with DNA bases results in atomic fragments, singly or multiply charged [8,9], whereas at very low ion energies they result in molecular fragment ions [10]. This suggests that the initial track distribution of secondary hyperthermal fragments, with different reactivities, will depend on the velocity of the primary ion, and thus its penetration depth in a biomedium; consequently the different damage caused by secondary fragments in the subsequent collision cascade will also depend on their initial distribution. Hence, more accurate dose models and radiation risk estimates must include not only the physical and physicochemical effects of the secondary fragments, but also their *initial distributions* along the heavy ion track.

This work is supported by NSERC of Canada, and the Canadian Space Agency; a NATO grant allowed staff travel to Sherbrooke (Ilko Bald).

*Corresponding author.
Electronic address: michael.huels@usherbrooke.ca
†Permanent address: Institut für Chemie-Physikalische und Theoretische Chemie, Freie Universität Berlin, Takustrasse 3, D-14195 Berlin, Germany.

[1] M. Goitein, A. J. Lomax, and E. S. Pedroni, Phys. Today **55**, No. 9, 45 (2002).
[2] D. Schulz-Ertner, A. Nikoghosyan, C. Thilmann, T. Haberer, O. Jäkel, C. Karger, G. Kraft, M. Wannenmacher, and J. Debus, Int. J. Radiat. Oncol. Biol. Phys. **58**, 631 (2004).
[3] M. Fuss, L. N. Loredo, P. A. Blacharski, R. I. Grove, and J. D. Slater, Int. J. Radiat. Oncol. Biol. Phys. **49**, 1053 (2001).
[4] M. Scholz, Nucl. Instrum. Methods Phys. Res., Sect. B **161–163**, 76 (2000).
[5] H. Stelzer, Nucl. Phys. B, Proc. Suppl. **61**, 650 (1998).
[6] S. Brons, G. Taucher-Scholz, M. Scholz, and G. Kraft, Radiat. Environ. Biophys. **42**, 63 (2003).
[7] M. Krämer and G. Kraft, Adv. Space Res. **14**, 151 (1994).
[8] J. de Vries, R. Hoekstra, R. Morgenstern, and T. Schlathölter, Phys. Rev. Lett. **91**, 053401 (2003).
[9] T. Schlathölter, R. Hoekstra, and R. Morgenstern, Int. J. Mass Spectrom. **233**, 173 (2004).
[10] Z.-W. Deng, I. Bald, E. Illenberger, and M. A. Huels, Phys. Rev. Lett. **95**, 153201 (2005).
[11] E. R. Benton and E. V. Benton, Nucl. Instrum. Methods Phys. Res., Sect. B **184**, 255 (2001).
[12] NASA Strategic Program Plan for Space Radiation Health Research (NASA, Washington, DC, 1998).
[13] S. B. Curtis, W. D. Hazelton, E. G. Luebeck, and S. H. Moolgavkar, Adv. Space Res. **34**, 1404 (2004).
[14] A. Arenz, C. E. Hellweg, M. M. Meier, and C. Baumstark-Khan, Adv. Space Res. **36**, 1680 (2005).
[15] Z.-W. Deng, I. Bald, E. Illenberger, and M. A. Huels (to be published).
[16] P. Rowntree, L. Parenteau, and L. Sanche, J. Phys. Chem. **95**, 4902 (1991); **95**, 523 (1991).
[17] Z.-W. Deng and R. Souda, J. Chem. Phys. **117**, 6235 (2002).
[18] E. Herceg, K. Mudiyanselage, and M. Trenary, J. Phys. Chem. B **109**, 2828 (2005).
[19] B. Willerding, W. Heiland, and K. J. Snowdon, Phys. Rev. Lett. **53**, 2031 (1984).
[20] X. Qin, T. Tzvetkov, X. Liu, D.-C. Lee, L. Yu, and D. C. Jacobs, J. Am. Chem. Soc. **126**, 13 232 (2004).
[21] M. A. Huels, L. Parenteau, and L. Sanche, J. Phys. Chem. B **108**, 16 303 (2004).
[22] I. Bald, Z.-W. Deng, E. Illenberger, and M. A. Huels, Phys. Chem. Chem. Phys. **8**, 1215 (2006).
[23] C. von Sonntag, *The Chemical Basis for Radiation Biology* (Taylor & Francis, London, 1987).
[24] V. Cobut, Y. Frongillo, J. P. Patau, T. Goulet, M.-J. Fraser, and J.-P. Jay-Gerin, Radiat. Phys. Chem. **51**, 229 (1998).
[25] B. Boudaïffa, P. Cloutier, D. Hunting, M. A. Huels, and L. Sanche, Science **287**, 1658 (2000).
[26] B. D. Michael and P. A. O'Neill, Science **287**, 1603 (2000).
[27] M. A. Huels, B. Boudaïffa, P. Cloutier, D. Hunting, and L. Sanche, J. Am. Chem. Soc. **125**, 4467 (2003).
[28] Y. Zheng, P. Cloutier, D. J. Hunting, J. R. Wagner, and L. Sanche, J. Am. Chem. Soc. **126**, 1002 (2004).
[29] K. Hieda, Int. J. Radiat. Biol. **66**, 561 (1994).